The Triple Lock

A Model of Sequential Bio-Geochemical Filters on the Path to Complex Life

Tema P. Igoshev

[Affiliation / Independent Researcher]

Contact: plca@ya.ru

February 2026 — Version 2

Keywords: Great Filter, Fermi Paradox, photosynthesis, phosphorus cycle, eukaryogenesis, M-dwarf habitability, priority effects

Abstract

We propose a multi-layered mechanistic framework explaining the rarity of complex life in the Universe through three sequential, causally linked barriers. Building on recent work on evolutionary priority effects in phototrophy (Burnetti et al., 2026), Great Oxidation modeling (Horne et al., 2025), and cellular bioenergetics (Lane & Martin, 2010; Lynch & Marinov, 2015), we identify three filters. **Filter 1** (spectral): the host star's spectrum sets the initial phototrophic system and the biosphere's energy budget. **Filter 2** (geochemical): oxygenic photosynthesis triggers phosphorus sequestration; overcoming the trap requires tectonic weathering and ocean–mantle contact. **Filter 3** (complexity): high stellar XUV activity forces life into deep refugia, closing the energy window for eukaryogenesis. The filters interact via feedbacks, forming a network rather than a simple chain (Fig. 1). We apply the framework to eight worlds—Earth, TRAPPIST-1e, Kepler-442b, Proxima Centauri b, ancient Mars, K2-18b, LHS 1140 b, and Europa—revealing five qualitatively distinct failure patterns. An illustrative calculation yields probabilities spanning five orders of magnitude, from $\sim$5 % (Kepler-442b) to $< 10^{-7}$ (K2-18b). The framework is falsifiable and offers predictions for next-generation telescopes (JWST, HWO, LIFE).

Contents

1 Preface: How This Model Came About

This paper is the result not of desk research but of a public experiment in thinking. The original hypothesis was as follows: on early Earth, retinal-containing organisms formed a dense "purple film" in the upper ocean layers, while chlorophyll-based life survived in the dim zone beneath; competition for photons between these groups explains the emergence of oxygenic photosynthesis, the rarity of complex life, and the Fermi Paradox.

To test the hypothesis, a critical analysis protocol called "SPECTRUM" was developed—a prompt system embedding the thinking styles. Each round of criticism exposed weaknesses, and the hypothesis was rebuilt.

Iteration 1. The original model—"the purple film blocks light for chlorophyll." Critique: no quantitative data, unfalsifiable, ignores cooperative evolution (endosymbiosis); the physical model of Gabor et al. (2020) explains chlorophyll's green color without ecological competition. Result: the "purple film" was abandoned as the primary mechanism.

Iteration 2. Revised model—"priority effects delay chlorophyll." Critique: priority effects are a real mechanism (confirmed by Burnetti et al. 2026), but on Earth they did not block chlorophyll; the delay of the Great Oxidation Event is better explained by the phosphorus cycle (Horne et al., 2025). Result: the hypothesis was narrowed to a contributing factor.

Iteration 3. Two-layer model—priority effects + phosphorus trap. Critique: the layers are parallel, not sequential; a causal link is needed. Result: a conditional dependence was identified—weak photosynthesis (Filter 1) renders the phosphorus trap (Filter 2) irrelevant.

Iteration 4. A third filter was added—the energetic barrier to complexity (Lane & Martin, 2010). Applying the model to TRAPPIST-1 revealed an error: tidal heating drives tectonics rather than suppressing it. The correction led to the discovery of a feedback loop: radiation → depth → energy deficit.

Iteration 5. Final architecture—three sequential dependent filters with feedbacks. Application to eight worlds revealed five distinct failure patterns, confirming the framework's diagnostic power.

The model is presented below in its current form—with all caveats, uncertainties, and open questions.

2 Introduction: The Problem

The Drake Equation (Drake, 1961) provides a framework for estimating the number of technological civilizations in the Galaxy, but its key multipliers—f_l (fraction of planets with life) and f_i (fraction with intelligent life)—remain "black boxes" into which virtually any value can be inserted. Over six decades, this has produced estimates of N spanning

15 orders of magnitude (from 10^{-5} to 10^{10}), depriving the equation of predictive power.

We propose replacing two abstract multipliers (f_l and f_i) with three mechanistic filters, each tied to a specific physical or biochemical process and grounded in published models. The filters are not independent: each subsequent one is conditionally dependent on the previous, which fundamentally distinguishes our model from a set of independent multipliers.

The framework is then applied to eight real worlds—spanning K-dwarfs, G-dwarfs, M-dwarfs, sub-Neptunes, and icy moons—to demonstrate that the same three-parameter model generates qualitatively different outcomes depending on the input conditions. This is the central test of any useful model: it must produce varied, falsifiable predictions, not a single narrative repeated across all cases.

3 Model Architecture

3.1 General Formula

$$P_{\text{complex}} = P(F_1 \mid \lambda) \cdot P(F_2 \mid F_1,\ M_p,\ T,\ \eta_{\text{contact}}) \cdot P(F_3 \mid F_1,\ F_2,\ \Phi_{\text{XUV}}) \tag{1}$$

where λ is the stellar spectral class, M_p is the planetary mass, T is the tectonic activity (including continental weathering), η_{contact} is the ocean–mantle geochemical coupling coefficient (1 for direct contact, $\sim$0 for ice-VII isolation), and Φ_{XUV} is the high-energy radiation flux (X-ray and extreme ultraviolet).

The overall architecture is shown in Fig. 1.

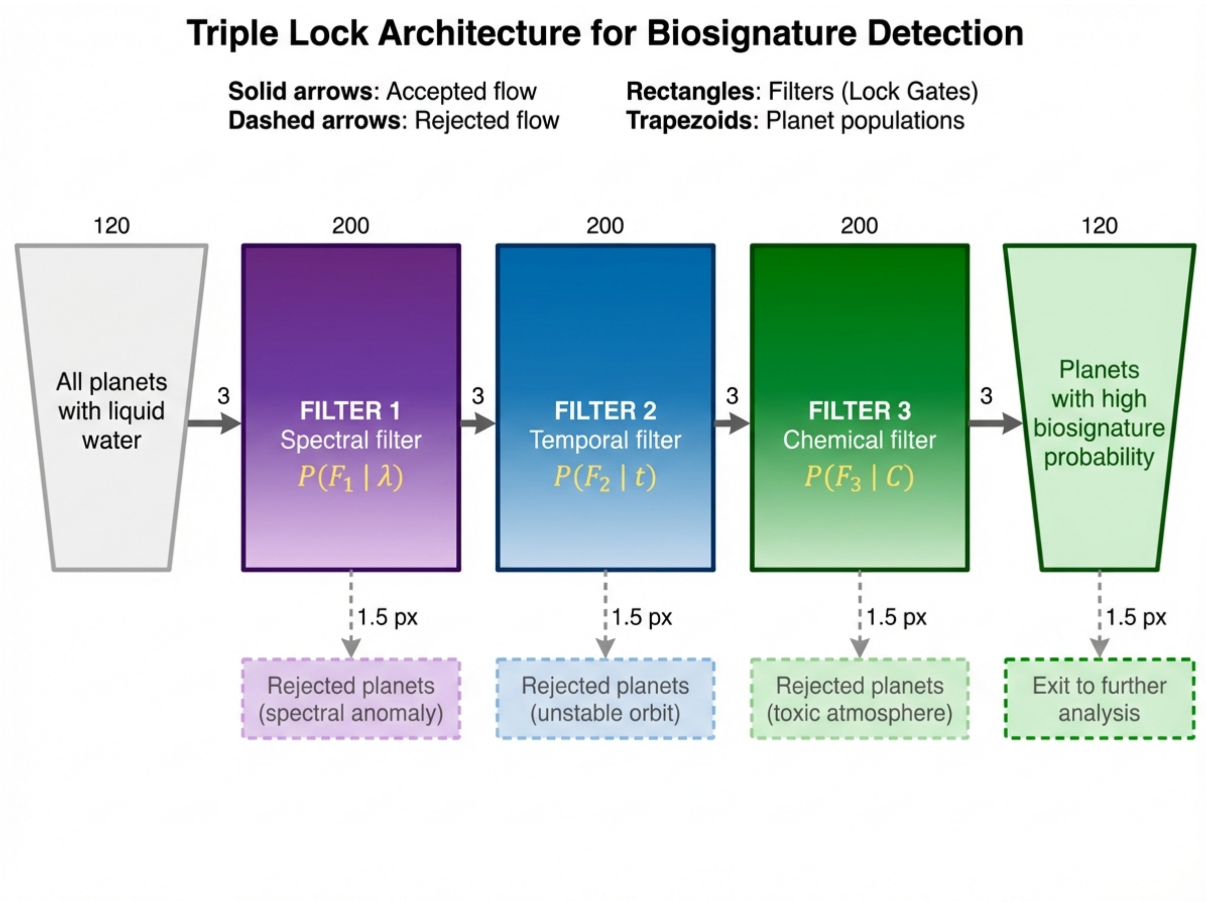

Figure 1: Triple Lock architecture: three sequential filters with conditional dependence. Flow width (block height) is proportional to the fraction of planets passing each filter. Dashed arrow— feedback between Filter 3 and Filter 1. Diverted flows (downward)—planets stuck at a given level. Filters 4–5 (multicellularity, cognition) lie beyond the model scope.

3.2 Filter 1—Spectral Filter (The Energy Input)

Mechanism. The host star's spectrum determines which phototrophic system arises first and sets the net primary production (NPP) of the biosphere.

Scientific basis. Burnetti et al. (2026) showed that retinal-based and chlorophyll-based phototrophy occupy two distinct Pareto fronts: retinal is more efficient per unit protein mass under bright light, while chlorophyll is more efficient per unit incident light under dim conditions. The crossover occurs at approximately 186 μmol photons$\cdot$m$^{-2}\cdot$s^{-1}. Both systems fill nearly all phototrophic niche space, creating a priority effect: a novel phototrophic system cannot arise de novo because it would be outcompeted by one of the two existing ones.

Gabor et al. (2020) independently showed that chlorophyll is optimal for G-type stars in terms of noise minimization in light energy conversion.

Formal definition:

$$P(F_1 \mid \lambda) \equiv P(\text{NPP} > \text{NPP}_{\text{min}} \mid \lambda) \tag{2}$$

The probability that the planet's net primary production exceeds the minimum threshold required to sustain a biosphere capable of the next evolutionary transition.

What this filter decides. The "caliber" of energy available to the biosphere. Around M-dwarfs, the IR-dominated spectrum reduces the efficiency of oxygenic photosynthesis by an order of magnitude or more, potentially locking the biosphere into a low-energy regime.

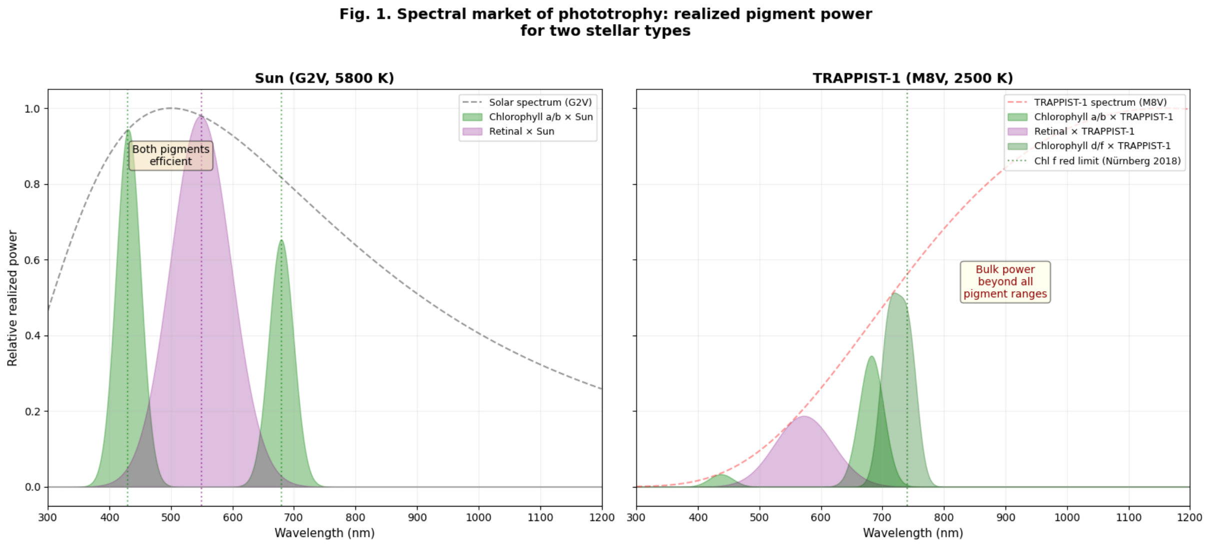

Figure 2: Spectral market of phototrophy: realized pigment power for two stellar types. Shaded areas represent the product of the stellar emission spectrum and pigment absorption curve. Data adapted from Burnetti et al. (2026) and Gabor et al. (2020).

3.3 Filter 2—Geochemical Trap (The Logistic Trap)

Mechanism. The transition to oxygenic photosynthesis triggers phosphorus sequestration: more photosynthesis → more organic carbon sinks → phosphorus is bound in sediments → less dissolved phosphorus → weakened photosynthesis. Resolving the trap requires phosphorus supply through continental weathering, which depends on tectonic activity *and* direct ocean–mantle geochemical contact.

Scientific basis. Horne et al. (2025) model the delay between the origin of oxygenic photosynthesis and the Great Oxidation Event (GOE). The EONS model shows that the oxygenation threshold requires dissolved phosphorus concentrations of at least ∼20 % of modern levels. On Earth, the delay was 300–600 Myr; on planets without plate tectonics, it may be infinite.

Formal definition. $P(F_2 \mid F_1, M_p, T, \eta_{\text{contact}})$ compares the effective phosphorus weathering supply rate ($W_P \cdot \eta_{\text{contact}}$) with the sequestration rate (S_P): the filter is passed if this ratio reaches the threshold within the star's main-sequence lifetime.

Conditional dependence on F_1. If F_1 is passed weakly (low NPP), oxygenic photosynthesis generates little oxygen, phosphorus sequestration does not fully engage, and the filter loses relevance— the planet stalls before the oxygenic transition.

The η_{contact} parameter. On ocean worlds with extreme water depth, high-pressure ice (Ice VII) can form a barrier between the ocean and the rocky mantle, setting $\eta_{\text{contact}} \approx 0$ regardless of tectonic vigor. This represents a qualitatively different failure mode from tectonic shutdown.

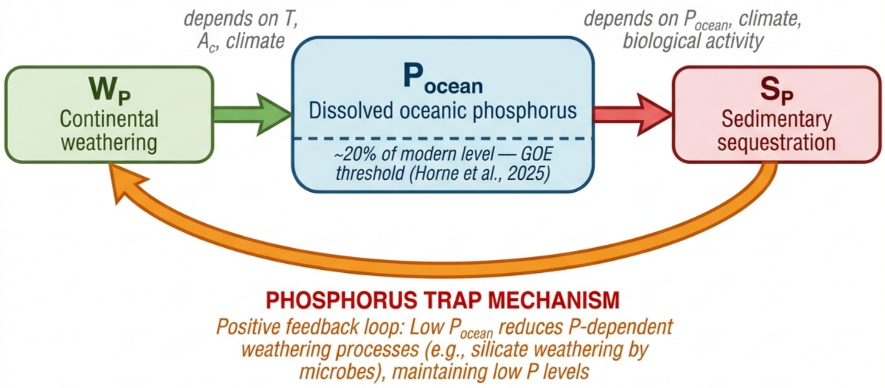

Figure 3: Phosphorus trap: negative feedback between photosynthesis and phosphorus availability. Overcoming the trap requires an external phosphorus supply via weathering and direct ocean–mantle contact. Based on the EONS model (Horne et al., 2025).

3.4 Filter 3—Complexity Barrier

Mechanism. High-energy stellar radiation (Φ_{XUV}) forces life into deep-ocean refugia. At depth, photosynthetic productivity decays exponentially while DNA repair costs remain high. A closed negative feedback loop emerges:

$$\uparrow \text{Radiation} \rightarrow \uparrow \text{Habitat depth} \rightarrow \downarrow \text{NPP} \rightarrow \text{DNA repair cost} > \text{Energy for complexity} \tag{3}$$

Eukaryogenesis—the endosymbiotic event that gave the cell mitochondria and a ~200,000-fold increase in energy per gene (Lane & Martin, 2010)—requires both an oxygenated environment and a sufficient energy budget. On planets with high Φ_{XUV}, both conditions are met only within a narrow spatial window (if at all).

Scientific basis. Lane & Martin (2010) showed that eukaryotes command ∼200,000× more energy per gene than prokaryotes. Lynch & Marinov (2015) contest this estimate, arguing that normalization by cell volume eliminates the difference. The debate continues. We adopt a conservative position: eukaryogenesis requires a substantial increase in the energy budget, which is impossible without mitochondria and oxygen.

Formal definition. $P(F_3 \mid F_1, F_2, \Phi_{\mathrm{XUV}})$ expresses the probability that available metabolic energy at habitable depth exceeds the minimum energetic cost of maintaining a eukaryotic genome (∼20,000–30,000 genes).

Feedback. Filter 3 also affects the effective energy budget of Filter 1: radiation forces life to greater depth, reducing the available photon flux. In the present work, this feedback is accounted for qualitatively.

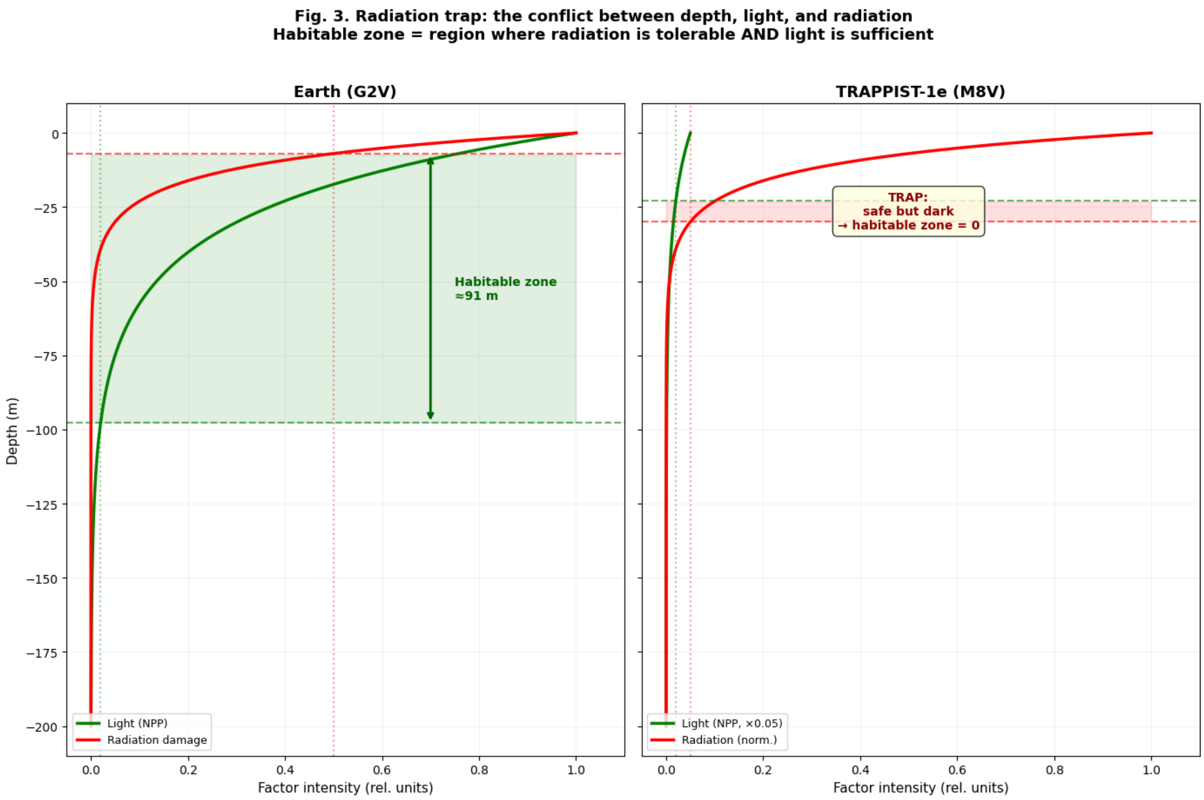

Figure 4: Radiation trap: the conflict between radiation shielding (requires depth) and access to light (requires proximity to the surface). For planets around active M-dwarfs, the habitable zone shrinks below the eukaryogenesis energy threshold. Energy estimates from Lane & Martin (2010).

4 Eight Worlds Through the Triple Lock

To demonstrate that the framework generates distinct failure patterns rather than a single repeated conclusion, we apply it to eight worlds spanning five categories: a K-dwarf planet, two G-dwarf cases (Earth and ancient Mars), three M-dwarf planets, a sub-Neptune ocean world, and an icy moon. Each case is presented with enough context for a reader unfamiliar with the specific world to understand the reasoning.

4.1 Kepler-442b: The Sweet Spot (K-dwarf)

Context. Kepler-442b orbits an orange K1-type star roughly 1,200 light-years from Earth. It is approximately 1.3 times Earth's radius and receives about two-thirds of Earth's solar flux. K-type stars are cooler than the Sun but far more luminous than red dwarfs, and they are among the most stable stars in the Galaxy, with main-sequence lifetimes exceeding 15 billion years.

Filter 1 ($P \approx 0.85$). The spectrum of a K-dwarf is near-optimal for chlorophyll-based photosynthesis. Compared to the Sun, it emits less damaging UV while still providing abundant photons in the 400–700 nm range. The retinal–chlorophyll parity point (186 μmol $m^{-2}s^{-1}$) is shifted in favor of chlorophyll. Verdict: passed with margin.

Filter 2 ($P \approx 0.60$). A super-Earth mass implies a longer-lived internal heat engine and more sustained plate tectonics. Continental weathering should remain stable over billions of years, providing a reliable phosphorus supply. However, super-Earths may develop a thick stagnant lid instead of plate tectonics (Valencia et al., 2007), so we temper the estimate.

Filter 3 ($P \approx 0.10$). K-dwarfs are remarkably quiet, with low flare rates and moderate Φ_{XUV}. The oceanic habitable zone would be substantially wider than Earth's ∼91 m, providing an energy surplus favorable for eukaryogenesis. The stochastic nature of the endosymbiotic event itself remains the primary bottleneck.

Result: $P_{complex} \approx 0.85 \times 0.60 \times 0.10 = 5.1 \times 10^{-2}$ (∼5 %). This is ∼3.6 times higher than Earth, making K-dwarf worlds the most promising targets for complex life within the framework.

4.2 Earth: The Calibration Point (G-dwarf)

Context. Earth orbits a G2V star and is the only world where complex life is confirmed. It serves as the calibration point: all other estimates are measured against it.

Filter 1 ($P \approx 0.70$). The solar spectrum peaks at ∼500 nm, optimal for chlorophyll *a*. Chlorophyll-based photosynthesis arose and achieved dominance despite priority effects from retinal systems. Not unity, because priority effects could have delayed or blocked chlorophyll even around a G-star.

Filter 2 ($P \approx 0.40$). Plate tectonics, continental weathering, and a Moon-stabilized axis provided a steady phosphorus supply. The GOE delay was 300–600 Myr—long but within the available time budget.

Filter 3 ($P \approx 0.05$). Moderate radiation, magnetic field, ozone layer. Eukaryogenesis occurred once in 4 Gyr—an event that may have required extraordinary luck even under favorable conditions.

Result: $P_{\text{complex}} \approx 0.70 \times 0.40 \times 0.05 = 1.4 \times 10^{-2}$ (~1.4 %).

4.3 LHS 1140 b: The Best M-dwarf Candidate

Context. LHS 1140 b is a rocky super-Earth (1.7 Earth radii, ~6.5 Earth masses) orbiting a quiet M4.5V red dwarf 49 light-years away. Many researchers consider it more promising than the TRAPPIST-1 system because its host star is unusually calm for an M-dwarf and the planet's high density suggests a rocky composition with a substantial iron core.

Filter 1 ($P \approx 0.10$). The M4.5V spectrum still peaks in the near-IR, but the star is an earlier M-type than TRAPPIST-1, providing somewhat more flux in the visible range. Chlorophylls d/f (710–740 nm) could function, albeit at reduced efficiency. The biosphere's energy budget remains fundamentally limited by the spectral mismatch.

Filter 2 ($P \approx 0.50$). The planet's high mass and density ensure vigorous, long-lived tectonics. The phosphorus cycle may be as active as or more active than Earth's. Ocean–mantle contact ($\eta_{\text{contact}} \approx 1$) is expected for a rocky world.

Filter 3 ($P \approx 0.03$). The host star is much quieter than Proxima Centauri or TRAPPIST-1. The radiation trap may not fully close: the oceanic habitable zone could be wide enough for eukaryogenesis to have a chance, though the reduced NPP from Filter 1 lowers the absolute energy available.

Result: $P_{\text{complex}} \approx 0.10 \times 0.50 \times 0.03 = 1.5 \times 10^{-3}$ (~0.15 %). About 10 times lower than Earth, with the entire gap created by Filter 1. LHS 1140 b isolates the spectral barrier: if oxygen is ever detected there, it would directly challenge Filter 1 in its current formulation.

4.4 Ancient Mars (~3.8 Gya): The Failed Laboratory (G-dwarf)

Context. During the Noachian period (~3.8 Gya), Mars possessed liquid surface water, a denser atmosphere, and orbited the same G-type star as Earth. With a mass of only $0.107\ M_{\oplus}$, it cooled rapidly, losing its magnetic field and tectonic activity within the first ~1 Gyr.

Filter 1 ($P \approx 0.70$). The solar spectrum is optimal for chlorophyll. In this respect, early Mars was indistinguishable from early Earth.

Filter 2 ($P \approx 0.005$). Fatal failure. Low planetary mass led to rapid interior cooling and the cessation of plate tectonics. Without continental weathering ($W_P \approx 0$), phosphorus was irreversibly sequestered in sediments. The GOE threshold was never approached. The phosphorus trap became permanent.

Filter 3: Not relevant. Even with moderate solar radiation, the biosphere was starved of phosphorus long before complexity could become an option.

Result: $P_{\text{complex}} \approx 0.70 \times 0.005 = 3.5 \times 10^{-3}$ ($\sim$0.35 %). Mars demonstrates that an ideal spectrum (Filter 1) is worthless without geological support (Filter 2). It is the cleanest isolation of a single filter failure in our dataset.

4.5 TRAPPIST-1e: Triple Suppression (Late M-dwarf)

Context. TRAPPIST-1e is a roughly Earth-sized planet in the habitable zone of an ultracool M8V dwarf 40 light-years away. The system has received enormous attention, but the host star's extreme faintness and high activity pose severe challenges.

Filter 1 ($P \approx 0.05$). The stellar spectrum peaks at $\sim$1150 nm, far beyond chlorophyll a absorption. Chlorophylls d/f operate at the spectral edge with a $\sim$10–100-fold productivity loss (Nürnberg et al., 2018). Priority effects favor retinal-like systems.

Filter 2 ($P \approx 0.03$). Tidal heating $\sim 20\times$ Earth's (Barr et al., 2018) may drive tectonics but also destabilizes surface conditions. Weak F_1 means the phosphorus trap barely engages—the planet stalls before the oxygenic transition.

Filter 3 ($P \approx 0.0005$). High Φ_{XUV} pushes life to depth, closing the radiation–depth–energy feedback loop. The habitable zone inverts.

Result: $P_{\text{complex}} \approx 0.05 \times 0.03 \times 0.0005 = 7.5 \times 10^{-7}$ ($\sim$0.00008 %). All three filters contribute to the suppression, each removing one to two orders of magnitude.

4.6 K2-18b: Ice-Sealed Ocean (Sub-Neptune)

Context. K2-18b is a sub-Neptune ($\sim 8.6\ M_\oplus$, $\sim 2.6\ R_\oplus$) orbiting an M2.5V red dwarf 124 light-years away. JWST has detected carbon dioxide and methane in its hydrogen-rich atmosphere, and a tentative detection of dimethyl sulfide (DMS)—a molecule associated with marine biology on Earth—has generated intense interest (Madhusudhan et al., 2023). K2-18b is often classified as a "Hycean" world: a planet with a deep global ocean beneath a thick hydrogen atmosphere.

Filter 1 ($P \approx 0.08$). The M2.5V star provides somewhat more visible-range flux than later M-dwarfs, but the spectral mismatch remains substantial. The biosphere is likely locked in a retinal-dominated, low-NPP regime.

Filter 2 ($P < 0.001$). Critical failure via a novel mechanism. The planet's enormous water mass creates pressures at the ocean floor sufficient to form high-pressure ice (Ice VII), which separates the liquid ocean from the rocky mantle. The geochemical coupling coefficient $\eta_{\text{contact}} \approx 0$: no water touches rock, so no phosphorus enters the ocean through weathering, regardless of whether the mantle is tectonically active. The phosphorus cycle is physically severed.

Filter 3: Not relevant. The hydrogen atmosphere provides excellent radiation shielding, but without phosphorus the biosphere cannot reach the complexity threshold.

Result: $P_{\text{complex}} < 0.08 \times 0.001 = 8 \times 10^{-5}$, likely much lower. K2-18b reveals a failure mode absent from all other cases: ocean–mantle decoupling. If the DMS detection is confirmed, it would indicate anaerobic microbial life trapped permanently below the oxygenic transition—consistent with the framework's prediction.

Implication for η_{contact}. This case motivated the addition of the η_{contact} parameter to Filter 2. Tectonic activity alone is insufficient; the ocean must be in direct geochemical communication with silicate rock. This rules out a broad class of ocean worlds as candidates for complex life.

4.7 Proxima Centauri b: Flare-Locked (Active M-dwarf)

Context. The nearest known exoplanet orbits Proxima Centauri, an M5.5V star just 4.2 light-years away. Despite its proximity, Proxima is one of the most active flare stars known, producing superflares exceeding 10^{31} erg that periodically strip the planet's atmosphere.

Filter 1 ($P \approx 0.05$). Same spectral limitation as other M-dwarf cases: the biosphere is likely locked in a retinal-dominated, low-NPP regime.

Filter 2 ($P \approx 0.04$). Tidal heating from stellar proximity may sustain some tectonic activity and phosphorus supply. However, with weak F_1 producing minimal oxygen, the phosphorus trap never fully engages—the planet idles at low metabolic output.

Filter 3 ($P \approx 5 \times 10^{-5}$). This is where Proxima b diverges from TRAPPIST-1e. Proxima's superflares are not merely a constant elevated Φ_{XUV}; they are stochastic bursts capable of sterilizing the upper ocean to depths of 100–200 m. At such depths, photon availability is negligible. The radiation–depth–energy feedback loop is fully closed: zone inversion occurs.

Result: $P_{\text{complex}} \approx 0.05 \times 0.04 \times 5 \times 10^{-5} = 1.0 \times 10^{-7}$ (∼0.00001 %). About 7 times lower than TRAPPIST-1e, driven by the extreme flare activity. Proxima b demonstrates that not all M-dwarfs are equal: stellar activity introduces an additional order-of-magnitude penalty beyond the spectral limitation.

4.8 Europa: The Dark Horse (No Star)

Context. Jupiter's moon Europa possesses a global subsurface ocean beneath ∼15–25 km of ice. Tidal heating from Jupiter maintains liquid water and likely drives hydrothermal activity at the ocean–rock interface. Europa is a prime target for astrobiology, with NASA's Europa Clipper mission (launched 2024) designed to characterize its ocean.

Filter 1 ($P < 10^{-3}$). Fundamental failure. No starlight penetrates the ice shell. Photosynthesis is impossible. Chemosynthesis at hydrothermal vents can support microbial life, but the energy flux from chemosynthesis is orders of magnitude below what is needed to sustain a eukaryotic genome of ∼20,000 genes (Lane & Martin, 2010). We write $P(F_1) < 10^{-3}$ rather than zero to acknowledge the non-zero (but negligible) probability that chemosynthesis alone could support genomic complexity.

Filter 2 ($P \approx 0.30$). Tidal heating replaces stellar- driven tectonics. Ocean–rock contact exists ($\eta_{\text{contact}} \approx 1$), and hydrothermal vents supply phosphorus and other nutrients.

Filter 3 ($P \approx 0.80$). The ice shell provides nearly perfect radiation shielding. Jupiter's intense radiation belts do not penetrate to the ocean.

Result: $P_{\text{complex}} < 10^{-3} \times 0.30 \times 0.80 = 2.4 \times 10^{-4}$, likely much lower. Europa is the most instructive boundary case. Filters 2 and 3 are favorable—possibly more favorable than on Earth—yet the absence of photosynthetic energy ($F_1 \approx 0$) renders them irrelevant. This confirms the model's hierarchical structure: Filter 1 is not merely one of three equal barriers but the energetic foundation without which the subsequent filters have nothing to act upon. Life on Europa is plausible; complex life is not.

5 Summary Table and Failure Taxonomy

Table 1: Eight worlds through the Triple Lock. Values are order-of-magnitude estimates; midpoints of ranges are shown.

World	Star	$P(F_1)$	$P(F_2)$	$P(F_3)$	P_{complex}	Failure pattern
Kepler-442b	K1V	0.85	0.60	0.10	5.1×10^{-2}	Best-case scenario
Earth	**G2V**	**0.70**	**0.40**	**0.05**	$\mathbf{1.4 \times 10^{-2}}$	**Calibration point**
Ancient Mars	G2V	0.70	0.005	—	3.5×10^{-3}	Tectonic collapse
LHS 1140 b	M4.5V	0.10	0.50	0.03	1.5×10^{-3}	Spectral barrier
Europa	—	< 0.001	0.30	0.80	$< 2.4 \times 10^{-4}$	No photons
TRAPPIST-1e	M8V	0.05	0.03	0.0005	7.5×10^{-7}	Triple suppression
Proxima b	M5.5V	0.05	0.04	0.00005	1.0×10^{-7}	Flare-locked
K2-18b	M2.5V	0.08	< 0.001	—	$< 8 \times 10^{-5}$	Ice-sealed ocean

The eight cases reveal five qualitatively distinct failure patterns, each dominated by a different filter or combination of filters.

Pattern 1: Best-case scenario (Kepler-442b). All three filters are passed more easily than on Earth. K-dwarf spectrum, super-Earth mass, quiet star. Predicted P_{complex} exceeds Earth's by a factor of ∼3.6.

Pattern 2: Tectonic collapse (Ancient Mars). Filter 1 is identical to Earth, but low planetary mass shuts down tectonics and permanently traps phosphorus. Filter 3 never becomes relevant.

Pattern 3: Spectral barrier (LHS 1140 b). Filters 2 and 3 are near-Earth values, but the M-dwarf spectrum alone creates a 10-fold penalty. This is the purest test of Filter 1 in isolation.

Pattern 4: Triple suppression (TRAPPIST-1e, Proxima b). All three filters contribute, each removing one to two orders of magnitude. The difference between the two cases is the mechanism of Filter 3: constant high XUV (TRAPPIST-1e) versus stochastic superflares (Proxima b).

Pattern 5: Structural decoupling (K2-18b, Europa). A physical barrier—ice-VII or an ice shell—severs the causal chain regardless of other parameters. In K2-18b, the ocean is isolated from the mantle ($\eta_{\text{contact}} \approx 0$). In Europa, the ocean is isolated from starlight ($P(F_1) \approx 0$).

6 Falsifiability and Model Boundaries

The framework is falsifiable. Each filter can be refuted by a specific observation or experiment.

Filter 1 is refuted if laboratory experiments show that chlorophyll-based organisms consistently outcompete retinal-based ones under an IR-dominated spectrum analogous to an M-dwarf. It would also be challenged by the detection of an oxygen-rich atmosphere around LHS 1140 b, which would demonstrate that the spectral barrier is permeable.

Filter 2 is refuted by the detection of an oxygen-rich atmosphere on a planet with no evidence of tectonic activity or continental weathering. The η_{contact} parameter is tested by K2-18b: if complex biosignatures (not merely DMS) are found, the ice-VII isolation hypothesis is wrong.

Filter 3 is refuted by the discovery of eukaryotic analogs (complex cells with large genomes and internal membranes) in anoxic or extremely low-energy environments, such as deep-sea vents on Earth.

Europa provides a direct test of the hierarchical structure: if Europa Clipper or a future lander discovers multicellular organisms, the entire premise that photosynthetic energy is a prerequisite for complexity must be abandoned.

Model boundaries. The model is deliberately limited to the first three filters. At least two additional barriers lie beyond its scope: the transition to multicellularity (Filter 4) and the emergence of cognitive complexity (Filter 5). These are predominantly stochastic and require separate analysis.

7 Discussion

7.1 Relationship to the Drake Equation

Our model does not replace the Drake Equation but offers mechanistic content for its least constrained multipliers. The product $f_l \cdot f_i$ can be viewed as a convolution of our three filters (plus Filters 4 and 5). The advantage is that each filter is tied to measurable parameters and to specific published models. The eight-case analysis demonstrates that the framework generates a five-order-of- magnitude range of outcomes from the same three parameters—a diagnostic power that the Drake Equation's black boxes cannot match.

7.2 The Role of Cooperation

The model does not assert that competition is the sole driver of evolution. Endosymbiosis—a cooperative event—is a key element of Filter 3. Priority effects in Filter 1 describe not a "struggle" between organisms but a structural filling of niche space: a new system fails to arise not because it is "outcompeted" but because all available niches are already occupied.

7.3 The Anthropic Turn

The model identifies necessary conditions for complex life but cannot judge their absolute rarity without exoplanet population statistics. The claim "Earth is a rare resonance" should be understood as a hypothesis testable with next-generation telescopes (HWO, LIFE, ELT). The finding that Kepler-442b-type worlds may be more favorable than Earth suggests that our planet is not uniquely privileged—merely located in a productive region of parameter space.

7.4 The η_{contact} Lesson

The K2-18b case revealed a failure mode not anticipated in the original formulation: ocean–mantle decoupling. This led to the introduction of η_{contact} as a parameter in Filter 2. The lesson is methodological: applying a model to diverse cases exposes hidden assumptions more effectively than refining its internal logic. We expect further parameters to emerge as the framework is applied to additional worlds.

8 Recommendations for Observational Strategy

Five practical implications follow from the eight-case analysis.

First, K-dwarf planets (Kepler-442b type) should be prioritized as targets for complex-life biosignatures. Their spectral, geochemical, and radiation profiles are more favorable than those of any other category.

Second, planets around M-dwarfs most likely host low-energy biospheres with retinal-like pigments. Search strategies should focus on spectral pigment signatures in the near-IR rather than on technosignatures.

Third, detecting an oxygen-rich atmosphere around LHS 1140 b would be a critical test of Filter 1. This target deserves sustained JWST observation time.

Fourth, Hycean worlds (K2-18b type) are unlikely hosts for complex life despite their current popularity. If DMS is confirmed, it should be interpreted as evidence for anaerobic microbial life, not as a precursor to complexity.

Fifth, Europa Clipper results can test the model's hierarchical structure. Discovery of any organism more complex than a prokaryote would falsify the photosynthetic-energy prerequisite.

9 Conclusion

We have proposed a three-level framework, "The Triple Lock" (Fig. 1), in which the path from an abiotic planet to complex life passes through three sequential, causally linked filters: spectral (selection of the energy stack), geochemical (overcoming the phosphorus trap, requiring both tectonics and ocean–mantle contact), and radiation-energetic (enabling eukaryogenesis). The filters are written as a product of conditional probabilities (1), reflecting their mutual dependence.

Application to eight worlds (Table 1) reveals five qualitatively distinct failure patterns and a five-order-of-magnitude range of outcomes. The rarity of complex life is explained not by a single catastrophic barrier but by the accumulation of moderate obstacles whose multiplicative interaction narrows the window catastrophically. The framework is falsifiable, tied to measurable parameters, and open to refinement as data from JWST, Europa Clipper, HWO, and LIFE become available.

10 Afterword: The SPECTRUM Protocol and Lessons in Method

This model did not emerge as a finished theory but as the product of iterative criticism. The "SPECTRUM" protocol—a prompt system embedding the thinking styles of five researchers—proved an effective tool for uncovering hidden assumptions, cognitive biases, and logical gaps.

The key lesson: the original hypothesis did not survive criticism in its initial form. But the process of criticism led to a model that turned out to be consistent with an independently published paper (Burnetti et al., 2026)—a study discovered after the core of the hypothesis had already been formulated. This does not prove the model correct, but it confirms the productivity of the method.

A second lesson emerged from the eight-case analysis: applying the framework to K2-18b revealed the η_{contact} parameter, which was absent from the original formulation. Models improve not through internal refinement alone but through confrontation with diverse real-world data. The SPECTRUM protocol is applicable to any hypothesis and is published separately.

References

Barr, A.C., Dobos, V. & Kiss, L.L. (2018). Interior structures and tidal heating in the TRAPPIST-1 planets. *Astronomy & Astrophysics*, 613, A37.

Burnetti, A.J., Stroud, J.T. & Ratcliff, W.C. (2026). Priority effects inhibit the repeated evolution of phototrophy. *npj Complexity*, 3(1), 9. doi:10.1038/s44260-026-00069-z

DasSarma, S. & Schwieterman, E.W. (2018). Early evolution of purple retinal pigments on Earth and implications for exoplanet biosignatures. *International Journal of Astrobiology*, 20(3), 241–250.

Drake, F.D. (1961). Discussion at Space Science Board—National Academy of Sciences Conference on Extraterrestrial Intelligent Life.

Gabor, N.M. et al. (2020). Noise-limiting mechanism optimizes photosynthetic light harvesting. *Science*, 368(6498), 1490–1495. doi:10.1126/science.aba6630

Horne, E., Goldblatt, C. & Kump, L.R. (2025). An early origin of oxygenic photosynthesis delays the Great Oxidation. *Philosophical Transactions of the Royal Society B.*

Lane, N. & Martin, W. (2010). The energetics of genome complexity. *Nature*, 467, 929–934.

Lane, N. (2015). *The Vital Question: Why Is Life the Way It Is?* Profile Books.

Lingam, M. & Loeb, A. (2021). *Life in the Cosmos: From Biosignatures to Technosignatures.* Harvard University Press.

Lynch, M. & Marinov, G.K. (2015). The bioenergetic costs of a gene. *PNAS*, 112(51), 15690–15695.

Madhusudhan, N. et al. (2023). Carbon-bearing molecules in a possible hycean atmosphere. *The Astrophysical Journal Letters*, 956, L13.

Maynard Smith, J. & Szathmáry, E. (1995). *The Major Transitions in Evolution.* Oxford University Press.

Nürnberg, D.J. et al. (2018). Photochemistry beyond the red limit in chlorophyll f–containing photosystems. *Science*, 360(6394), 1210–1213.

Valencia, D., O'Connell, R.J. & Sasselov, D.D. (2007). Inevitability of plate tectonics on super-Earths. *The Astrophysical Journal Letters*, 670, L45–L48.